LabVIEW-based laser frequency stabilization system with phase-sensitive detection servo loop for Doppler LIDAR applications

John A. Smith
Xinzhao Chu
Wentao Huang
Johannes Wiig
University of Colorado at Boulder
Cooperative Institute for Research in
    Environmental Sciences
    and
Department of Aerospace Engineering Sciences
216 UCB
Boulder, Colorado 80309
E-mail: Xinzhao.Chu@Colorado.edu

Archie T. Brown
Triad Technology, Inc.
P.O. Box 1853
Longmont, Colorado 80502

Abstract. Resonance fluorescence Doppler lidars using Doppler shift and spectral broadening effects are the principal instruments to simultaneously measure wind and temperature in the middle atmosphere. Such lidars demand high accuracy, precision, and stability of the laser optical frequency. Current resonance Doppler lidars suffer various problems in frequency stabilization that limit their locking precision and stability. We have addressed these problems by developing a LabVIEW®-based laser frequency locking system. This new system utilizes wavelength-modulation and phase-sensitive-detection techniques in conjunction with a proportional-integral-derivative feedback servo loop. It achieves better than ±1-MHz locking precision and stability over 1 h. The system also remains locked throughout a series of abrupt disturbance tests. Owing to its high locking precision, immunity to electronic and laser noise, reliability, and flexibility in adapting for various systems, we believe that this new system represents a marked improvement in resonance Doppler lidar technology. © *2008 Society of Photo-Optical Instrumentation Engineers.* [DOI: 10.1117/1.3013257]

Subject terms: phase-sensitive detection; laser frequency stabilization; lidar; LabVIEW; saturation-absorption spectroscopy; wavelength modulation; lock-in amplifier.

Paper 080521R received Jul. 2, 2008; revised manuscript received Sep. 4, 2008; accepted for publication Sep. 9, 2008; published online Nov. 10, 2008.

1 Introduction

Various types of Doppler lidars rely on Doppler shift and broadening effects to measure wind and temperature from the lower to the upper atmosphere. Among them, the resonance fluorescence (Na and K) Doppler lidars provide a unique means to measure the mesosphere and lower thermosphere (MLT)—the least-understood atmospheric region.[1] Narrowband Na and K Doppler lidars require the frequency of a continuous wave (cw) seed laser to be locked to one of the Doppler-free features of a Na or K vapor cell.[1–3] Such frequency locking not only stabilizes the output frequency, but also provides an absolute frequency calibration for the entire lidar system, enabling wind measurements. High accuracy, precision, and stability (over hours) are demanded in the laser frequency (within 1 MHz) in order to achieve high measurement accuracy. However, current Na and K Doppler lidars suffer various problems in laser frequency locking that limit the measurement accuracy.

Originally, in resonance fluorescence lidar, locking a cw seed laser frequency to a known reference (e.g., a peak or a dip of atomic absorption lines) was accomplished using a *direct intensity comparison* method via software.[1,2] A drawback to this method is its susceptibility to large laser and background intensity fluctuations, resulting in low locking precision and stability (~5 to 10 MHz). A variant of this direct intensity comparison, the *scan-then-hold* method, ex-

periences even worse problems in that the laser frequency may fluctuate without compensation in between scans. Implementing a dedicated hardware-based phase-sensitive detection (PSD) servo loop improved the locking precision to a certain degree;[3] however, this hardware was sensitive to electromagnetic interference. The hardware PSD was also inflexible, and one locker box could only work with one particular laser. Historically, saturation-fluorescence spectroscopy was chosen over saturation-absorption spectroscopy for lidar frequency locking, but the inferior signal-to-noise ratio (SNR) resulted in low locking stability, especially for K spectroscopy.

We have addressed these issues by developing a laser frequency stabilization system based on National Instruments LabVIEW® software (version 8.2). This new locking system utilizes PSD technology with a unique filtering technique and a proportional-integral-derivative (PID) servo loop in conjunction with Doppler-free saturation-absorption spectroscopy.[4,5] This simple system achieves better than ±1 MHz of precision and stability over an hour, and is nearly immune to noise, since signals are handled digitally. Because it is a software implementation, its settings can be easily modified for different lasers and/or control systems. The laser locking technology was developed and tested on an 852-nm external cavity diode laser (ECDL), locking to cesium (Cs), and was applied to lock a 770-nm ECDL to the potassium (K) D_1 line for improving K Doppler lidar performance. The Cs D_2 transitions at 852.335 nm were chosen as our test bed, since the spectroscopic peaks from a Cs vapor cell are very distinct
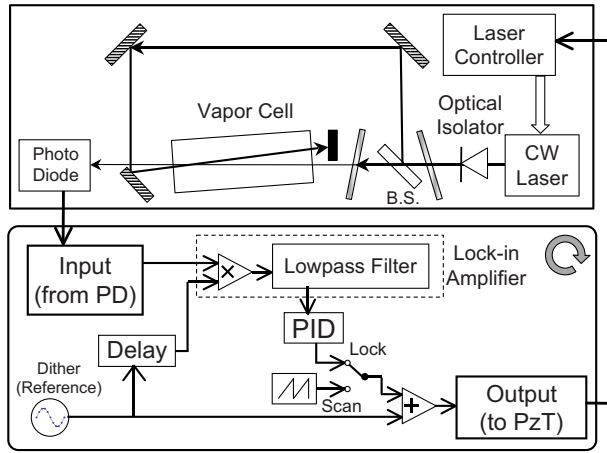
Fig. 1 Experimental setup for saturation-absorption spectroscopy (top) and a schematic diagram of the software locking system (bottom). Pump and probe powers are measured at the entrance to the vapor cell.

Fig. 2 A front panel screen shot of the LabVIEW locking program during a scan on Cs with derivative (top) and spectrum (bottom) signals recorded simultaneously.

at room temperature and well separated from one another.[4] Accommodating any other atomic species (e.g., Na, K, Rb), however, would only require adjusting the operating temperature of the vapor cell and the center wavelength of the laser.

In the following, we introduce the methodology and then present test results on both Cs and K laser locking to demonstrate the effectiveness and robustness of this new system. Conclusions and proposed future improvements are given at the end.

2 Methods

2.1 *Experimental Setup*

Figure 1 illustrates the experimental setup, including the Doppler-free saturation-absorption spectroscopy setup (top) and the software-based PSD and PID servo loop (bottom). Our experimental studies show that saturation-absorption spectroscopy provides superior SNR to saturation-fluorescence spectroscopy[4] for two main reasons. First, while fluorescence spectroscopy only collects photons from a portion of the cell, absorption spectroscopy utilizes the full length of a vapor cell, leading to more distinct Doppler-free features. Second, the transmitted laser intensity is higher than the ambient background light, thus providing higher SNR in the photon detection process. More distinct Doppler-free features and higher SNR help achieve better locking precision and short-term stability, making the saturation-absorption spectroscopy (see Fig. 2) a better choice for laser frequency stabilization. A vapor cell with wedged windows is preferred in the experiment; however, a normal vapor cell with straight windows can be slightly tilted to avoid multiple reflections for achieving better Doppler-free resolution.

The test lasers are ECDLs (Triad Technology 2010A) with a Littman-Metcalf design, tuned with piezoelectric transducers (PzTs). The laser wavelengths are monitored by a wavemeter (Burleigh WA-1500) to 0.1-pm precision (not shown in Fig. 1). After passing through an optical isolator, the laser beam is split into a pump and probe for saturation-absorption spectroscopy. Gradient neutral-density filters
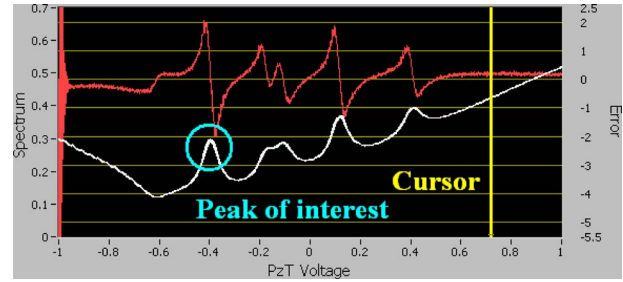
situated before and after the beamsplitter allow adjustment of the pump and probe powers for optimization between shot noise and power broadening [Cs: 910 (27) μW pump (probe); K: 237 (16) μW pump (probe)].[6] The output of a photodiode (with a sensitivity of 184 mV/μW at 852 nm and 224 mV/μW at 770 nm) behind the pump mirror that detects the probe beam transmission is coupled to an analog 18-bit input channel on the data acquisition (DAQ) board (National Instruments Multifunction DAQ PCI-6281). The PzT tuning input of the laser controller (Triad Technology 2010A) has been modified for unity gain and coupled to the analog output channel of the DAQ board.

2.2 *Computer Realization of Locking Servo Loop*

To lock the laser to one of the Doppler-free peaks, a discriminant signal must be generated to tell the control system in which direction and how far to drag the laser. Following the wavelength modulation spectroscopy (WMS) technique,[7] the laser frequency is modulated at 1 kHz by adding a small sinusoidal signal to the PzT bias voltage. A lock-in amplifier is required for WMS to generate the derivative signals that provide both phase and amplitude information, telling the control system the direction and magnitude of required corrections, respectively. A single-channel, single-phase lock-in amplifier is emulated in LabVIEW software to fulfill this role. A mathematical treatment of WMS and PSD is covered in various works[5,7–10] and duplicated here to detail the working principle.

By dithering the PzT bias voltage we modulate the laser frequency ω at

$$\omega = \omega_0 + m \sin \omega_m t, \tag{1}$$

where ω_0 is the original laser frequency, m is the modulation amplitude, ω_m is the modulation frequency, and t is time. The transmitted laser intensity I_T through the vapor cell may be written as

$$I_T(\omega) = I_T(\omega_0 + m \sin \omega_m t). \tag{2}$$

We take $m \ll \Gamma$ and $\omega_m \ll \Gamma$ for WMS, where Γ is the linewidth of the saturation-absorption peak. Thus, I_T can be expanded as a Taylor series:

$$I_T(\omega) = I_T(\omega_0) + m\sin\omega_\mathrm{m}t\frac{\mathrm{d}I_T}{\mathrm{d}\omega} + \frac{m^2\sin^2\omega_\mathrm{m}t}{2!}\frac{\mathrm{d}^2I_T}{\mathrm{d}\omega^2}$$

$$+ \frac{m^3\sin^3\omega_\mathrm{m}t}{3!}\frac{\mathrm{d}^3I_T}{\mathrm{d}\omega^3} + \cdots. \tag{3}$$

We use trigonometric identities to simplify Eq. (3) and then combine terms to obtain

$$I_T(\omega) = \left[I_T(\omega_0) + \frac{m^2}{4}\frac{\mathrm{d}^2I_T}{\mathrm{d}\omega^2} + \cdots\right] + \sin\omega_\mathrm{m}t\left[m\frac{\mathrm{d}I_T}{\mathrm{d}\omega}\right.$$

$$\left. + \frac{m^3}{8}\frac{\mathrm{d}^3I_T}{\mathrm{d}\omega^3} + \ldots\right] + \cos 2\omega_\mathrm{m}t\left[-\frac{m^2}{4}\frac{\mathrm{d}^2I_T}{\mathrm{d}\omega^2} + \cdots\right]$$

$$+ \cdots. \tag{4}$$

Therefore, the transmitted intensity contains a dc term and terms oscillating at ω_m, $2\omega_\mathrm{m}$, and so on. Since the modulation is sufficiently small ($m \ll \Gamma$), the first term in each bracket is dominant. For the transmitted intensity $I_T(\omega)$ that has peaks with Gaussian shape (like Doppler-limited absorption lines) or Lorentzian shape (like Doppler-free saturation-absorption lines), the odd derivatives $\mathrm{d}^{2n+1}I_T(\omega)/\mathrm{d}\omega^{2n+1}$ possess linear zero crossings about each peak, making them suitable as locking discriminants. The photodiode signal of the transmitted intensity is multiplied (mixed) with the dither (reference) signal as below for homodyne detection of the odd derivatives in the $\sin\omega_\mathrm{m}t$ term of Eq. (4):

$$I_T(\omega) \times \sin\omega_\mathrm{m}t = \sin\omega_\mathrm{m}t\left[I_T(\omega_0) + \frac{m^2}{4}\frac{\mathrm{d}^2I_T}{\mathrm{d}\omega^2} + \cdots\right]$$

$$+ \sin^2\omega_\mathrm{m}t\left[m\frac{\mathrm{d}I_T}{\mathrm{d}\omega} + \frac{m^3}{8}\frac{\mathrm{d}^3I_T}{\mathrm{d}\omega^3} + \ldots\right]$$

$$+ \sin\omega_\mathrm{m}t\cos 2\omega_\mathrm{m}t\left[-\frac{m^2}{4}\frac{\mathrm{d}^2I_T}{\mathrm{d}\omega^2} + \cdots\right]$$

$$+ \cdots. \tag{5}$$

Utilizing the trigonometric identity $\sin^2\omega_\mathrm{m}t = (1-\cos 2\omega_\mathrm{m}t)/2$, we obtain

$$I_T(\omega) \times \sin\omega_\mathrm{m}t = \frac{1}{2}\left[m\frac{\mathrm{d}I_T}{\mathrm{d}\omega} + \frac{m^3}{8}\frac{\mathrm{d}^3I_T}{\mathrm{d}\omega^3} + \cdots\right]$$

$$+ \sin\omega_\mathrm{m}t\left[I_T(\omega_0) + \frac{m^2}{4}\frac{\mathrm{d}^2I_T}{\mathrm{d}\omega^2} + \cdots\right]$$

$$- \frac{1}{2}\cos 2\omega_\mathrm{m}t\left[m\frac{\mathrm{d}I_T}{\mathrm{d}\omega} + \frac{m^3}{8}\frac{\mathrm{d}^3I_T}{\mathrm{d}\omega^3} + \ldots\right]$$

$$+ \frac{1}{2}(\sin 3\omega_\mathrm{m}t - \sin\omega_\mathrm{m}t)\left[-\frac{m^2}{4}\frac{\mathrm{d}^2I_T}{\mathrm{d}\omega^2}\right.$$

$$\left. + \cdots\right] + \cdots. \tag{6}$$

Recognizing that the dc term given by the first bracket in Eq. (6) is proportional to the odd derivatives and there are many other unwanted terms oscillating at ω_m, $2\omega_\mathrm{m}$, $3\omega_\mathrm{m}$, etc., we then filter the mixed signal (6) with a lowpass filter
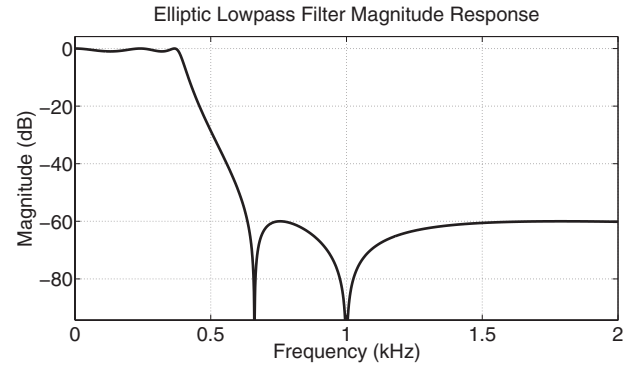

Fig. 3 The magnitude response of the filter with a lowpass cutoff at 387 Hz, showing large attenuation at the dither frequency (1 kHz).

(Fig. 3) to pass the dc term while attenuating all higher harmonic oscillating terms. The result is the dominant first derivative (i.e., the error signal). Screen shots for both Cs and K spectroscopy and the derivatives are presented in Figures 2 and 4, respectively.

The preceding process iterates continuously on a computer with both input and output channels clocked at 15 kHz. The photodiode return signal is multiplied with the phase-delayed 1-kHz reference sine wave in a point-by-point fashion. The mixed signal is then filtered by a software-realized, fifth-order elliptic lowpass filter with a 60-dB stop band and very large attenuation at 1 kHz to comb out the first-harmonic response—where the most filtering is required (see Fig. 3). This lock-in amplification results in an error signal. The error signal is then fed to a PID controller for conversion to an appropriate incremental correction voltage that is output to the PzT for laser frequency corrections. Figure 5 illustrates a pseudocode representation of the control algorithm employed in the Lab-VIEW program.

To reduce the noise and improve the SNR, a very narrowband lowpass filter is desired. Naturally, a narrow bandwidth entails a large time constant, causing slow servo response. Therefore, a trade-off exists between the lowpass filter bandwidth and the system response time. The filter parameters shown in Fig. 3 reflect this trade-off. The modulation frequency ω_m should be far from any major noise frequency ω_noise (close to dc in our system), so the frequency-mixing process in Eq. (6) will shift the noise from low frequency to the difference and sum frequencies ($|\omega_\mathrm{m} \pm \omega_\mathrm{noise}|$). Since $|\omega_\mathrm{m} \pm \omega_\mathrm{noise}|$ are far from the dc term, noise can be removed with ease.

3 Results

Our system is designed specifically for ease of use and flexibility. The graphical user interface (GUI) is shown in Fig. 4. A routine initiates a laser frequency scan after clicking the SCAN button and displays the resulting spectrum with an overlay of the obtained derivative signal to assist the user in choosing the locking point and optimizing various parameters. Afterwards, locking is simply a matter of dragging a cursor (straight vertical line on the GUI) to or near the desired peak and toggling the SCAN button to LOCK to engage the servo loop. Users can easily modify
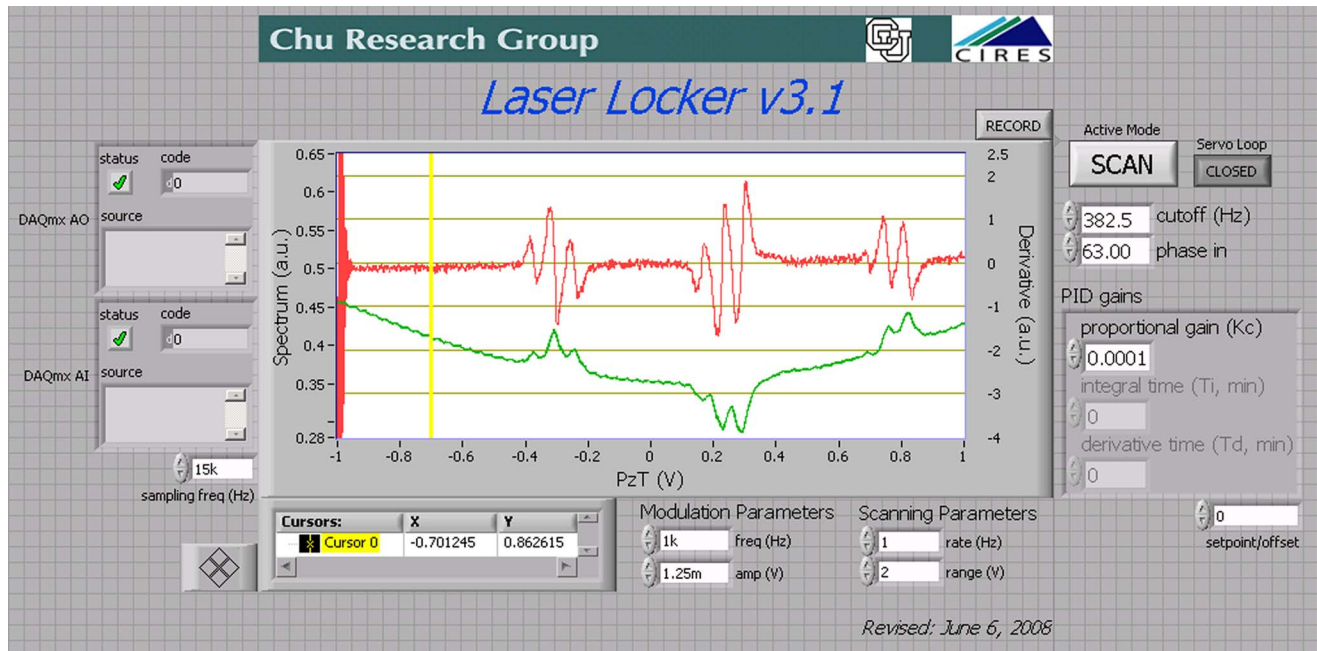
Fig. 4 Graphical user interface (GUI) for the laser frequency locking system after scanning the potassium spectrum.

servo loop parameters (like modulation frequency and amplitude, and filter and PID parameters) on the GUI for different application needs.

An indication of a working lock to a desired peak is an apparent doubling of the dither frequency appearing in the photodetected transmission—the so-called 2-f signal. The upper waveforms in Fig. 6 illustrate this 2-f signal, recorded by an oscilloscope, averaged over 128 synchronized 5-ms snapshots during a lock to the peak of interest (marked in Fig. 2). Averaging greatly reduces the detector

Fig. 5 Pseudocode representation of the control algorithm for laser frequency stabilization in flow-chart format. RSS: reference sinusoidal signal.

noise, clearly revealing the 2×1-kHz signal. With the 2-f signal and the mean transmitted intensity at the desired peak height, it is shown that the laser frequency is stabilized at the apex of the correct peak in the spectrum. Below we present the test results on locking precision, disturbance rejection, and long-term locking stability.

3.1 Locking Precision Estimate

How to estimate locking precision is a valid question for all laser frequency stabilization systems. For our system we notice that the 2-f signal is always seen throughout the locking period, indicating that the laser central (carrier) frequency is within the modulation amplitude surrounding the apex throughout locking. This can be better explained from Fig. 7 which illustrates the Lorentzian line shape of the Doppler-free peak and how the 1-f dither signal results in a 2-f photodetected transmission signal around the apex. Only when the laser central frequency deviates from the peak more than one modulation amplitude will the 2-f signal disappear from the photodetected transmission signal. Estimating the locking precision with the modulation amplitude provides an upper limit for the central-frequency deviation. However, considering that the dither itself is a disturbance to the laser frequency, the modulation amplitude is indeed a good estimate of the laser frequency locking precision.

The PzT bias voltage is dithered directly, as shown in Fig. 6 (lower waveforms). To estimate the locking precision, this dither voltage must be converted to the modulation amplitude in frequency [the m in Eq. (1)—also called the modulation depth]. This conversion has to take into account the nonlinear response of the PzT tuning element at high modulation frequencies like 1 kHz. When the PzT is scanned very slowly, the wavelength calibration curve shown in Fig. 8 provides a conversion between the PzT
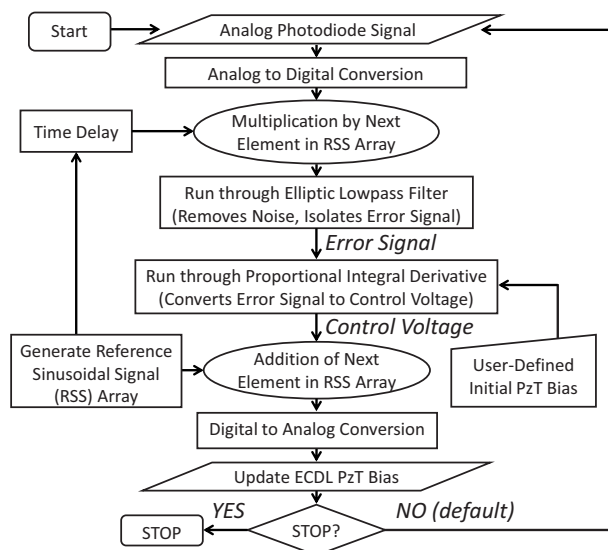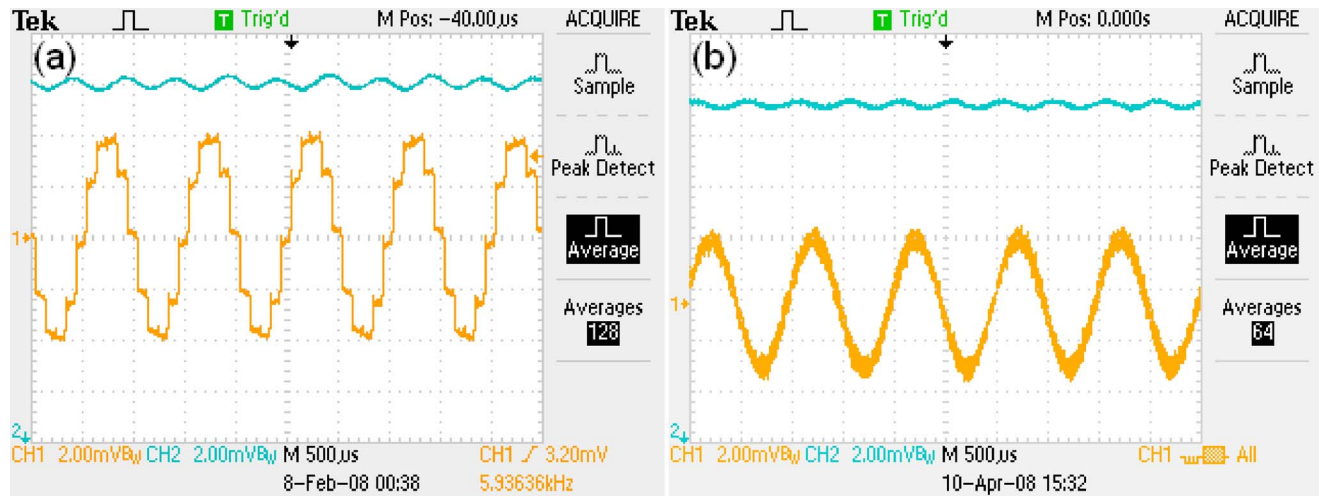
Fig. 6 (a) A recorded 2-f photodetected transmission signal (top) resulting from a 5-mV modulation (bottom) during lock for Cs. (b) Similar case for K, but from a 3-mV modulation.

scan voltage and laser carrier frequency detuning, which shows a nearly linear response of 344 MHz/V for Cs and 438 MHz/V for K. However, the same response cannot be assured at higher modulation rates. An appropriate approach is to derive the modulation amplitude from the 2-f signal amplitude and the corresponding spectral peak. First, a slow-scan Doppler-free peak spectrum was taken immediately before locking (Fig. 7). Based on physical considerations of the peak of interest, a model of the Lorentzian line shape with tilted background was fitted to the data points:
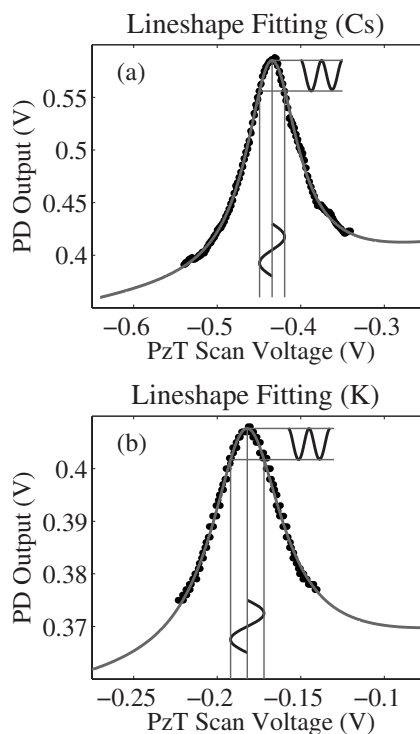
Fig. 7 A Lorentzian line-shape model for (a) Cs and (b) K spectral peaks, used to retrieve the modulation depth, fitted to the desired peak with an exaggerated dither to show the predicted 2-f response.
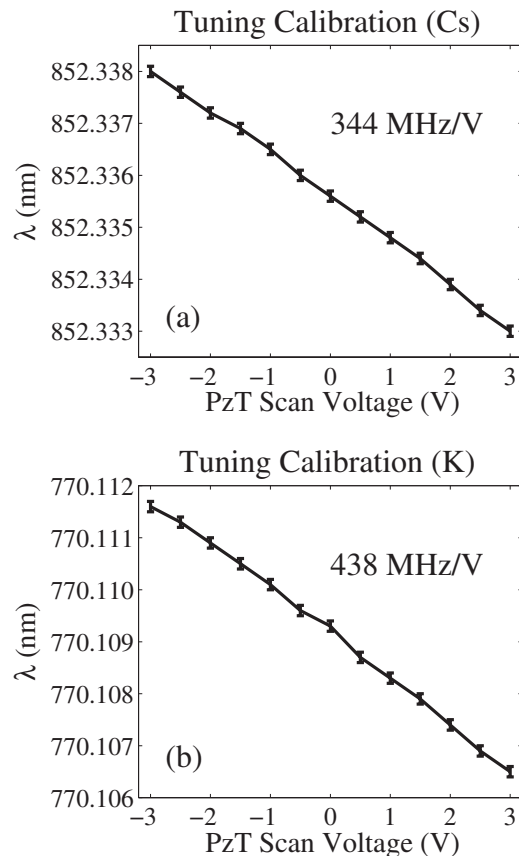

Fig. 8 Laser output wavelength recorded by the wavemeter versus the PzT scan voltage; used to calculate the relationship between laser frequency detuning and scan voltage: (a) Cs and (b) K.

Table 1 Fitting parameters for Lorentzian line-shape fit given by Eq. (7).

Parameter	Cesium	Potassium
A (V^2)	0.0039	5.81×10^{-4}
γ (V)	0.0755	0.0526
ω_0 (V)	−0.4343	−0.1825
C (V)	0.4258	0.371
k	0.1083	0.0494

$$V_{PD} = \frac{A\gamma}{(\gamma/2)^2 + (x - \omega_0)^2} + C + kx, \qquad (7)$$

where V_{PD} is the photodiode output voltage representing the transmitted laser intensity through the vapor cell, x is the PzT dither voltage representing the laser frequency change, A is a constant for the Lorentzian peak, γ is the Lorentzian linewidth (FWHM), ω_0 is the frequency corresponding to the peak, C is a constant pedestal, and k is the slope of the tilted background due to the Doppler-broadened background absorption. The obtained parameters for both Cs and K are tabulated in Table 1. Second, the 2-f signal peak-to-peak amplitudes are measured by oscilloscope. They are 0.5 and 0.15 mV, respectively, for Cs and K. We then use the Lorentzian fitted model to predict the modulation amplitude (voltage) in a slow scan that would produce the observed 2-f amplitude (Fig. 7). The obtained 1-f amplitudes are 1.65 mV for both Cs and K. Finally, using the slow-scan wavelength calibration curves in Fig. 8, we calculate the modulation amplitude (depth) as

344 MHz/V × 1.65 mV = 0.57 MHz   (for Cs),

438 MHz/V × 1.65 mV = 0.72 MHz   (for K).

Based on the preceding analyses, we estimate the laser frequency locking precision from the modulation amplitudes to be ±0.6 and ±0.75 MHz for Cs and K, respectively.

3.2 Disturbance Rejection Tests
Besides locking precision, immunity from disturbance and long-term stability of the laser frequency locking are critical features for lidar applications. Disturbance rejection trials were conducted to test the ability of the system to remain locked after an abrupt disturbance. The photodetected transmission signal was monitored during a series of disturbance events, such as knocking on the optical bench. During three disturbance events, as shown in Fig. 9, the transmission signal (upper waveform) returns persistently to the original level within a fraction of a second, indicating a persistent recovery to the peak of interest despite a strong disturbance. The lower waveform in Fig. 9 shows the control output voltage and how it reacts to drag the laser frequency back to the peak.
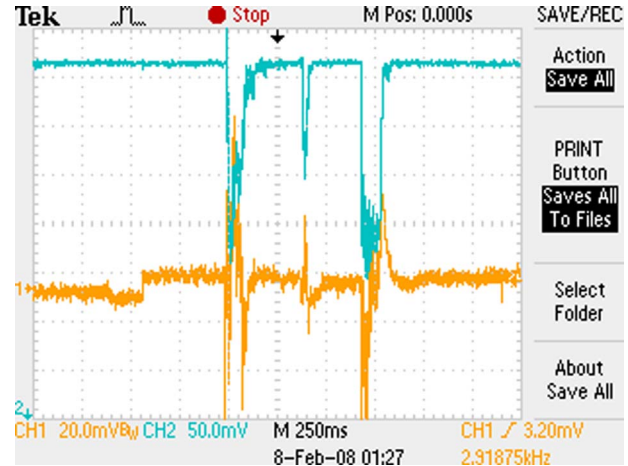

Fig. 9 Photodiode return (top) and control output (bottom) to show the locking system response to three disturbance events. The return of the photodiode signal to a constant dc level indicates a persistent recovery.

We also tested the locking system response to ambient light intensity changes, to simulate a common disturbance event. A flashlight was shined on the detecting photodiode, and a large response in the photodetected return was observed, as expected. However, once the flashlight was removed, the 2-f waveform returned to its original dc level, indicating that the laser frequency had remained locked to the desired peak. This result is very encouraging—the phase-sensitive detection technique demonstrates much less susceptibility to intensity changes than the direct intensity comparison methods. Therefore, even if the laser intensity or the vapor cell pressure changes during the lock, causing the transmission intensity (photodiode returns) to fluctuate, the PSD-based servo loop can still function to lock the laser frequency to the desired peak. Ac detection in PSD, in contrast with dc, is immune to intensity noise for time scales long compared to the modulation. This feature is important for long-term lidar observations when laser intensity variations are unavoidable during multiple hours of operation.

3.3 Long-Term Locking Stability Tests
Tests on locking stability were conducted to measure the magnitude of frequency excursion and drift from the peak over an extended period. The output of the lock-in amplifier (error signal) is perhaps the most reliable measure of stability, since it attempts to isolate physical shifts in the laser carrier frequency from ambient noise. Following a familiar technique,[11,12] the error signal was sampled once per second for a period of one hour undisturbed during a lock (Fig. 10). Error, the lock-in amplifier output, is a measure of the magnitude and direction of frequency deviation from the peak. Error signal samples were within approximately ±0.1 and ±0.08 error (arbitrary unit) from zero for Cs and K, respectively, in the trials. Fluctuations in the error signals were interpreted as shifts in the laser carrier frequency,[11,12] and a model of the discriminant (Fig. 11), again based on physical considerations of the peak of interest, allowed us to convert between error signal units and detuning voltage. The discriminant can be approximated as a linear function
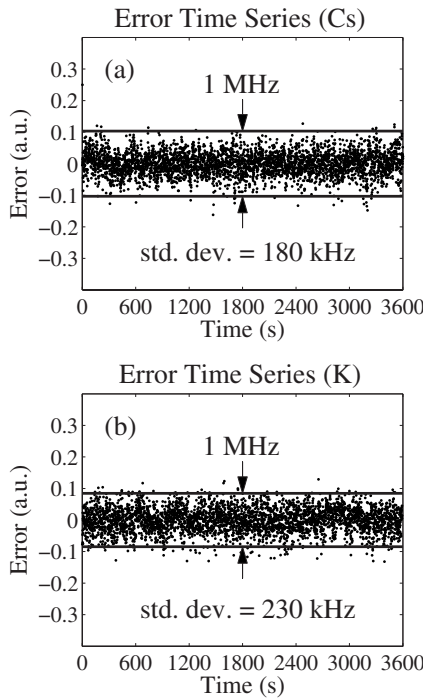
Error Time Series (Cs)

Error Time Series (K)

Fig. 10 Error signal sampled over time: (a) Cs and (b) K.

near zero with a slope of 71 Error/V for Cs and 74 Error/V for K, respectively. Thus the frequency excursions during the tests are estimated as
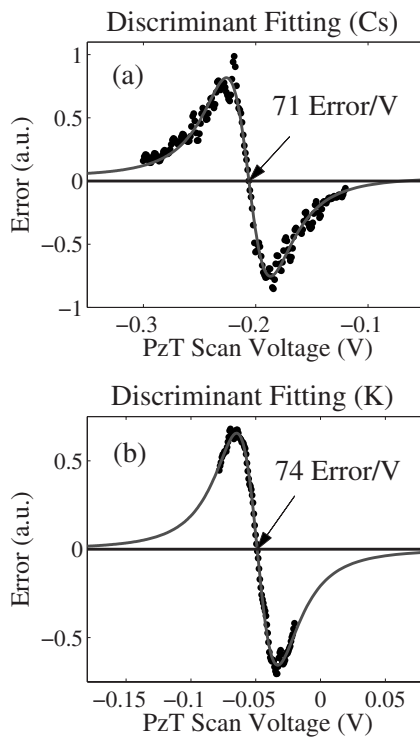
Discriminant Fitting (Cs)

Discriminant Fitting (K)

Fig. 11 A model of the discriminant from which the magnitudes of frequency excursions about the peak are estimated: (a) Cs and (b) K.
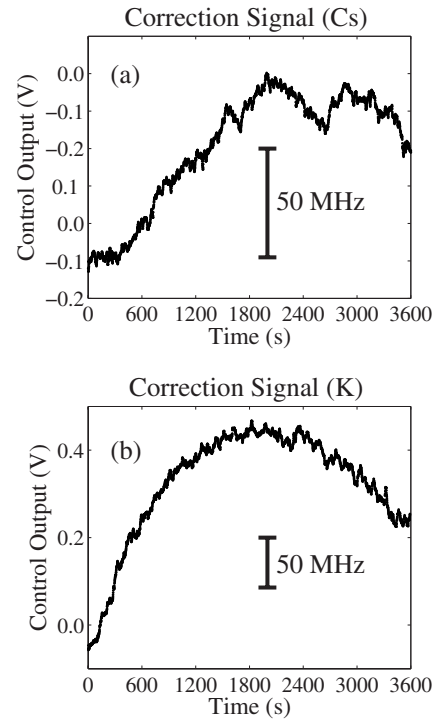
Correction Signal (Cs)

Correction Signal (K)

Fig. 12 PID control voltage output recorded over time to show the frequency drift, were the servo loop disengaged. The lack of discontinuities indicates a sustained lock. (a) Cs and (b) K.

$$\frac{344 \text{ MHz/V}}{71 \text{ Error/V}} \times (\pm 0.1 \text{ Error}) = \pm 0.5 \text{ MHz} \qquad \text{(for Cs)},$$

$$\frac{438 \text{ MHz/V}}{74 \text{ Error/V}} \times (\pm 0.08 \text{ Error}) = \pm 0.5 \text{ MHz} \qquad \text{(for K)}.$$

Therefore, the locking stability is statistically within approximately ± 0.5 MHz from the apex throughout this hour-long trial. Taking account of frequency excursion and modulation yields an overall uncertainty of ± 1.0 MHz for the laser frequency locking precision and stability.

Figure 12 is a record of the servo loop PID output voltage to the PzT during the hour-long trials, illustrating how the servo loop continuously compensates the diode laser cavity frequency to track the Doppler-free peak. This long-term drift can be attributed to diode base temperature variations. No abrupt changes occur, indicating no loss of lock during the trails.

A high-precision and high-speed wavelength meter with 0.5 MHz of precision at 770 nm (HighFinesse WSU-2) was recently acquired. A wavelength (frequency) measurement of the 770-nm ECDL laser frequency locked to a K vapor cell using this wavelength meter over an extended period demonstrates that the locking precision and stability are within ± 1 MHz (Fig. 13), in agreement with our previous test results. The drift in Fig. 13 is attributable to changes in wavelength-meter temperature.

4 Conclusions and Outlook

We have demonstrated a LabVIEW-based laser frequency stabilization system. This system utilizes wavelength-
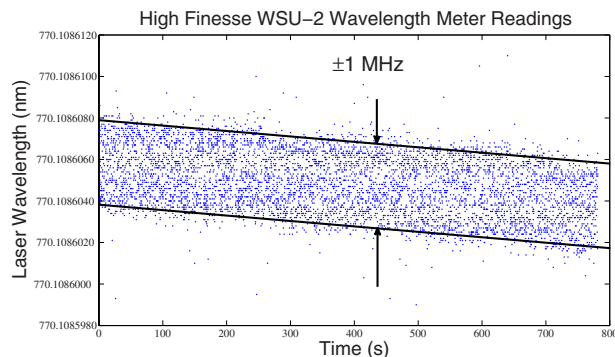
Fig. 13 Wavelength-meter-measured frequency precision and stability when the servo loop is engaged.

modulation and phase-sensitive-detection techniques in conjunction with a PID servo loop to lock external cavity diode lasers precisely, stably, and reliably to one of the Doppler-free saturation-absorption features of Cs and K. Our test results show that the laser frequency locking precision and stability are within ±1.0 MHz during hour-long tests. In addition, the system is able to stay locked throughout a series of disturbance events. In view of this feature, coupled with an easy graphical user interface and greater flexibility, we believe that our frequency locking system represents a marked improvement in laser frequency stabilization for resonance Doppler lidars.

Future work will concentrate on applying the locking system to a ring dye laser using a Na vapor cell as a reference. The ring dye laser is the master oscillator for the current Na Doppler lidars.[1] This LabVIEW-based system is expected to significantly improve the Na Doppler lidar frequency-locking precision, stability, and reliability. Later improvements may include multiple harmonic detection and a MATLAB-Simulink model to help select PID parameters. More advanced features are also desirable in lidar applications, e.g., warning users when the lock has been lost or when locking performance has degraded, and auto-search of the spectroscopic peaks after the lock was lost.

This project is an effort by the Consortium Technology Center (CTC), operating under the umbrella of the Consortium of Resonance and Rayleigh Lidars (CRRL) funded by the National Science Foundation. CTC will make the locking code available to the community on request.
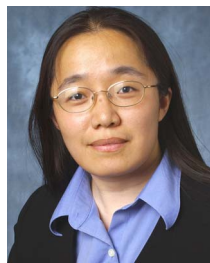
References

1. X. Chu and G. Papen, "Resonance fluorescence lidar for measurements of the middle and upper atmosphere," in *Laser Remote Sensing*, T. Fujii, and T. Fukuchi, Eds., pp. 179–432, CRC Press (2005).
2. C. Y. She, J. R. Yu, H. Latifi, and R. E. Bills, High-spectral-resolution fluorescence light detection and ranging for mesospheric sodium temperature measurements, *Appl. Opt.* **31**, 2095–2106 (1992).
3. J. S. Friedman, C. A. Tepley, S. Raizada, Q. H. Zhou, J. Hedin, and R. Delgade, "Potassium Doppler-resonance lidar for the study of the mesosphere and lower thermosphere at the Arecibo Observatory," *J. Atmos. Sol.-Terr. Phys.* **65**, 1411–1424 (2003).
4. X. Chu, W. Huang, J. S. Friedman, and A. T. Brown, "CRRL/CTC: Doppler-free saturation-absorption and polarization spectroscopy for resonance fluorescence Doppler lidars," in *Proc. 24th Int. Laser Radar Conf. (ILRC)*, pp. 809–812 (2008).
5. W. Demtröder, *Laser Spectroscopy*, Springer (2003).
6. T. Ikegami, S. Sudo, and Y. Sakai, *Frequency Stabilization of Semiconductor Laser Diodes*, Artech House (1995).
7. J. Supplee, E. Whittaker, and W. Lenth, "Theoretical description of frequency modulation and wavelength modulation spectroscopy," *Appl. Opt.* **33**, 6294 (1994).
8. R. W. P. Drever, J. L. Hall, F. V. Kowalski, J. Hough, G. M. Ford, A. J. Munley, and H. Ward, "Laser phase and frequency stabilization using an optical resonator," *Appl. Phys. B* **31**, 97–105 (1983).
9. G. C. Bjorklund, M. D. Levenson, W. Lenth, and C. Ortiz, "Frequency modulation (FM) spectroscopy: theory of lineshapes and signal-to-noise analysis," *Appl. Phys. B* **32**, 145–152 (1983).
10. New Focus, "FM spectroscopy with tunable diode lasers," Application Note 7, New Focus, San Jose, CA (2007).
11. G. Koch, "Automatic laser frequency locking to gas absorption lines," *Opt. Eng.* **42**, 1690–1693 (2003).
12. G. Koch, A. Cook, C. Fitzgerald, and A. Dharamsi, "Frequency stabilization of a diode laser to absorption lines of water vapor in the 944-nm wavelength region," *Opt. Eng.* **40**, 525–528 (2001).

John A. Smith received his BS degree in engineering physics from the Colorado School of Mines in 2006. He is now working towards his MS in aerospace engineering sciences at the University of Colorado at Boulder. His research includes digital laser frequency stabilization with applications to lidar remote sensing of the atmosphere. Mr. Smith will continue into the PhD program on completion of his master's, focusing on advancements in lidar instrumentation and applications therein.

Xinzhao Chu is currently an associate professor in the Department of Aerospace Engineering Sciences, University of Colorado at Boulder (UCB). She is a fellow of the Cooperative Institute for Research in Environmental Sciences. She received her BS and PhD degrees in physics and electrical engineering from Peking University in 1991 and 1996, respectively. During her tenure at the University of Illinois at Urbana-Champaign from 1997 to 2005, she made the first pole-to-pole lidar measurements of the middle and upper atmosphere in 1999–2001. She published "Resonance fluorescence lidar for measurements of the middle and upper atmosphere" in the book *Laser Remote Sensing* in 2005. Now she teaches a graduate-level lidar course at UCB, and serves as the director of Consortium Technology Center for the national Consortium of Resonance and Rayleigh Lidars. Dr. Chu is the principal investigator for the National Science Foundation Major Research Instrumentation mobile Fe-resonance Rayleigh-Mie Doppler lidar.
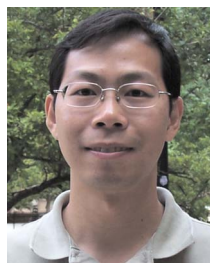
Wentao Huang is currently a research scientist in the Cooperative Institute for Research in Environmental Sciences (CIRES), University of Colorado at Boulder. He received his BS and PhD degrees in physics and optics in the field of nonlinear optics and ultrafast time-resolved spectroscopy from Peking University (Beijing, China) in 1998 and 2003, respectively. Afterward he worked as a postdoctoral research associate in physical chemistry in the Department of Chemistry, University of Illinois at Urbana-Champaign. He joined CIRES in 2006, and has been working on innovative lidar technology, laser spectroscopy, and atmospheric science since then.

Johannes Wiig is conducting graduate studies towards a PhD degree in the Department of Aerospace Engineering Sciences at the University of Colorado, where he is majoring in remote sensing. Before beginning the PhD program in Boulder, he worked as a space and atmospheric analyst at the Arecibo Observatory (2005) and a satellite controller at the Swedish Space Corporation (2004). He also held a research assistantship at the Penn State University (2003) and a consultant position in the Southwest Research Institute Space Science Department (2000). Current degrees held by Mr. Wiig are a MSc in space technology from Umea University Space Science Department and a BSc in space engineering, also from the Umea University in Sweden. He is a sergeant in the Swedish Royal Army.
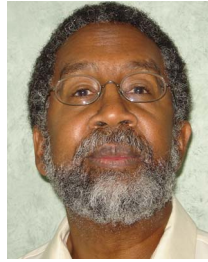
Archie T. Brown is the founder and vice president of operations at Triad Technology, Inc, based in Boulder, Colorado. Triad Technology is a supplier of atomic and molecular reference cells and spectroscopy instrumentation. Mr. Brown received a BS from Southern Methodist University and an MS from the University of Texas in electrical engineering. He was a cofounder of several start-up companies. He was a cofounder and the CEO at Environmental Optical Sensors, Inc. (EOSI), a manufacturer of external cavity diode laser systems. Mr. Brown has more than 20 years of experience with the design of electronic subsystems used in temperature, current, and wavelength stabilization of laser-diode-based systems.